Intestinal epithelial cell-derived IL-15 determines local maintenance and maturation of intraepithelial lymphocytes in the intestine

AUTHOR(S):

Zhu, Yuanbo; Cui, Guangwei; Miyauchi, Eiji; Nakanishi, Yuki; Mukohira, Hisa; Shimba, Akihiro; Abe, Shinya; ... Seno, Hiroshi; Ohno, Hiroshi; Ikuta, Koichi

CITATION:

Zhu, Yuanbo ...[et al]. Intestinal epithelial cell-derived IL-15 determines local maintenance and maturation of intraepithelial lymphocytes in the intestine. International immunology 2020, 32(5): 307-319

ISSUE DATE:

2020-05

URL:

http://hdl.handle.net/2433/250992

Intestinal epithelial cell-derived IL-15 determines local maintenance and maturation of intraepithelial lymphocytes in the intestine

Yuanbo Zhu,[1,2] Guangwei Cui,[1] Eiji Miyauchi,[3] Yuki Nakanishi,[5] Hisa Mukohira,[1,2] Akihiro Shimba,[1] Shinya Abe,[1,2] Shizue Tani-ichi,[1,6] Takahiro Hara,[1] Hiroshi Nakase,[7] Tsutomu Chiba,[8] Atsuko Sehara-Fujisawa,[9] Hiroshi Seno,[5] Hiroshi Ohno,[3,4,10] and Koichi Ikuta[1]

[1]Laboratory of Immune Regulation, Department of Virus Research, Institute for Frontier Life and Medical Sciences, Kyoto University, Kyoto 606-8507, Japan

[2]Graduate School of Medicine, Kyoto University, Kyoto 606-8501, Japan

[3]Laboratory for Intestinal Ecosystem, RIKEN Center for Integrative Medical Sciences, Yokohama 230-0045, Japan

[4]Division of Immunobiology, Department of Medical Life Science, Graduate School of Medical Life Science, Yokohama City University, Yokohama 230-0045, Japan

[5]Department of Gastroenterology and Hepatology, Graduate School of Medicine, Kyoto University, Kyoto 606-8507, Japan

[6]Laboratory of Biological Chemistry, Human Health Sciences, Graduate School of Medicine, Kyoto University, Kyoto 606-8507, Japan

[7]Department of Gastroenterology and Hepatology, Sapporo Medical University, School of Medicine, Sapporo 060-8543, Japan

[8]Kansai Electric Power Hospital, Osaka 553-0003, Japan

[9]Laboratory of Tissue Stem Cell Biology, Department of Regeneration Science and Engineering, Institute of Frontier Life and Medical Sciences, Kyoto University, Kyoto 606-8507, Japan

[10]Kanagawa Institute of Industrial Science and Technology, Kanagawa 213-0012, Japan

Correspondence:

Koichi Ikuta

53 Shogoin-Kawaharacho, Sakyo-ku

Kyoto 606-8507, JAPAN

E-mail: ikuta.koichi.6c@kyoto-u.ac.jp; TEL: 075-751-4012; FAX: 075-751-4810.

Running title: Role of IL-15 in gut intraepithelial lymphocytes

Keyword: Bcl-2, colitis, microbiota, microenvironment.

Abbreviations used: Ab, antibody; BEC, blood vascular endothelial cell; DC, dendritic cell; DSS, dextran sodium sulfate; IEC, intestinal epithelial cell; IEL, intestinal intraepithelial lymphocyte; IELP, IEL precursor; IL, interleukin; Tie2-Cre, tie2 promoter-driven Cre; Vil-Cre, villin promoter-driven Cre.

Abstract

Interleukin-15 (IL-15) is a cytokine critical for maintenance of intestinal intraepithelial lymphocytes (IELs), especially CD8αα$^+$ IELs (CD8αα IELs). In the intestine, IL-15 is produced by intestinal epithelial cells (IECs), blood vascular endothelial cells (BECs) and hematopoietic cells. However, the precise role of intestinal IL-15 on IELs is still unknown. To address the question, we generated two kinds of IL-15 conditional knockout (IL-15cKO) mice: villin-Cre (Vil-Cre) and Tie2-Cre IL-15cKO mice. IEC-derived IL-15 was specifically deleted in Vil-Cre IL-15cKO mice, whereas IL-15 produced by BECs and hematopoietic cells is deleted in Tie2-Cre IL-15cKO mice. The cell number and frequency of CD8αα IELs and NK IELs were significantly reduced in Vil-Cre IL-15cKO mice. By contrast, CD8αα IELs were unchanged in Tie2-Cre IL-15cKO mice, indicating that IL-15 produced by BECs and hematopoietic cells is dispensable for CD8αα IELs. Expression of an anti-apoptotic factor, Bcl-2, was decreased, whereas Fas expression was increased in CD8αα IELs of Vil-Cre IL-15cKO mice. Forced expression of Bcl-2 by a Bcl-2 transgene partially restored CD8αα IELs in Vil-Cre IL-15cKO mice, suggesting that some IL-15 signal other than Bcl-2 is required for maintenance of CD8αα IELs. Furthermore, granzyme B production was reduced, whereas PD-1 expression was increased in CD8αα IELs of Vil-Cre IL-15cKO mice. These results collectively suggested that IEC-derived IL-15 is essential for homeostasis of IELs by promoting their survival and functional maturation.

Introduction

IL-15 is a cytokine essential for development, homeostasis and function of memory CD8 T cells, NK cells, NKT cells and intestinal intraepithelial lymphocytes (IELs). IL-15 receptor consists of three subunits: the common cytokine receptor γ-chain (γc), the shared IL-2R β-chain (IL-2Rβ) and a unique IL-15R α-chain (IL-15Rα). Apart from other cytokines, IL-15 functions through a unique mechanism known as trans-presentation, in which IL-15Rα bound to IL-15 (IL-15/IL-15Rα complex) is presented to recipient cells expressing the γc and IL-2Rβ. IL-15 can be produced by various cell types such as bone marrow stromal cells, thymic epithelial cells, blood and lymphatic endothelial cells, dendritic cells (DCs), macrophages and intestinal epithelial cells (IECs) (1).

Intestine is constantly exposed to environmental stimuli such as microbiota and food antigens. IELs together with IECs form the first line of defense in the intestine. IELs mainly consist of T cells and are divided into two major types: conventional and unconventional IELs. $CD4^{+}TCR\alpha\beta^{+}$ and $CD8\alpha\beta^{+}TCR\alpha\beta^{+}$ cells are termed as conventional IELs and are progenies of conventional T cells activated by foreign antigens in the periphery. Other IELs, either $TCR\alpha\beta^{+}$ or $TCR\gamma\delta^{+}$, lack CD4 and express CD8αα homodimers and are termed as unconventional IELs. They acquire their activated phenotype by recognizing self-antigens during development in thymus. The development and function of unconventional IELs have been long-standing issues. Unlike conventional IELs, unconventional IELs tend to be immune suppressive and exert regulatory functions (2). They highly express activating and inhibitory types of NK cell receptors and thus are characterized as activated yet resting immune cells (3). Nevertheless, these unconventional IELs are rich in cytolytic granules, facilitating them to respond to invasions rapidly. While no specific function of

CD8αα^{+}TCRαβ^{+} IELs has been described yet, TCRγδ^{+} IELs can restore the integrity of the epithelium under injuries by secreting keratinocyte growth factor (4).

IL-15 is essential for IELs, as CD8αα IELs are severely reduced in IL-15$^{-/-}$, IL-15Rα$^{-/-}$ and IL-2Rβ$^{-/-}$ mice (5-7). So far, roles of IL-15 on IELs have been studied in vitro and in vivo by using IL-15$^{-/-}$ or IL-15Rα$^{-/-}$ mice. IL-15 supports the survival of CD8αα IELs through up-regulating their Bcl-2 expression (8-11). In addition, IL-15 controls the development of CD8αα^{+}TCRαβ^{+} IELs through T-bet (12) and regulates the generation of TCR repertoire of TCRγδ^{+} IELs (13). As IEL precursors (IELPs) originate from thymus and reside in intestine as mature CD8αα IELs, it is unclear from where and how they receive IL-15 signals. Furthermore, bone marrow transplantation experiment showed that unconventional IELs depend on parenchymal cell-produced IL-15Rα and IL-15 (14). Consistently, Vil-Cre IL-15Rα$^{fl/fl}$ mice showed similar deficiency in CD8αα IELs to IL-15$^{-/-}$ mice (15). Besides, NK cells are also exist in intestinal intraepithelial region, and IL-15 is critical for their survival, proliferation, maturation and activation (15-17). However, IL-15 is produced by intestinal epithelial cells, DCs, macrophages and endothelial cells in the intestine (1). Thus, the source of IL-15 essential for IELs is yet to be clarified.

To elucidate the precise role of intestinal IL-15 on IELs, we generated IL-15-floxed mice and crossed them with villin- or tie2-promoter-driven Cre (Vil-Cre or Tie2-Cre) transgenic mice to establish conditional knockout of IL-15 (IL-15cKO) in IECs or BECs/hematopoietic cells, respectively. We found that the absolute numbers of CD8αα^{+} IELs are significantly decreased and the functional maturation is impaired in Vil-Cre IL-15cKO mice, but unchanged in Tie2-Cre IL-15cKO mice. Whereas, the absolute numbers of NK IEL are also reduced in Vil-Cre IL-15cKO mice. Taken together, these observations indicate that IEC-derived IL-15 plays an essential role in the development and maintenance of IELs and implies that IEC provide a unique IL-15 niche for IELs.

Materials and Methods

Mice

IL-15-floxed mice were generated in our lab and will be reported elsewhere. Vil-Cre Tg mice were obtained from the Jackson Laboratory (18). H2K-Bcl-2 Tg mice were reported previously (19). All mice used in this study were from a C57BL/6 background and were maintained under specific pathogen-free conditions at the Experimental Research Center for Infectious Diseases in the Institute for Frontier Life and Medical Sciences, Kyoto University. All mouse experiments were approved by the Animal Research Committee in Kyoto University. Male or female littermates were analyzed at 8–12 weeks of age.

Cell preparation

IECs were isolated from mouse small intestine as previously reported (20). Briefly, 1cm long tissue was dissected from the small intestine and soaked in Hanks' balanced salt solution containing 30 mM EDTA. After incubation on ice for 10 min, epithelial sheet was isolated with a fine needle. The epithelium sheet was disaggregated into single cell suspension of IEC by pipetting. BECs ($gp38^{-}CD31^{+}$) were isolated from mouse small intestine as previously reported (21).

IELs were isolated from small intestine and colon as described previously (22). In brief, small intestine was flushed and turned inside-out with the aid of polyethylene tubing. The inverted intestine was cut into 3 segments and fastened with strings. All sections were transferred into a 50 mL tube containing 40 mL Hanks' balanced salt solution with 5% fetal bovine serum and 10 mM Hepes (pH7.4). The tube was shaken horizontally at 37℃ for 45 min at 150 rpm. The tissue suspension was passed through a 40 μm strainer and centrifuged for 10 min at 270 × g. Cell pellet was suspended in 30% Percoll and centrifuged at 620 × g for

20 min to deplete epithelial cells. The cell pellet was then resuspended in 40% Percoll, underlaid with 70% Percoll, and centrifuged at 620 × g for 20 min. IELs from the interface between 40% and 70% Percoll layers were collected, washed and resuspended in phosphate buffered saline with 1% bovine serum albumin and 0.05% sodium azide.

LPLs were prepared as previously reported with slight modification (23). In brief, after Peyer's patches were excised, the intestine was opened longitudinally and incubated 30 min in PBS with 5 mM EDTA at 37℃ to remove epithelial cells. After incubation, intestine was washed with PBS to fully remove epithelial cells and debris. The remaining tissue was cut into small pieces and transferred into a 50 mL tube containing RPMI1640 medium with 5% FBS, 1.25 mg/ml collagenase D (Roche) and 50 μg/ml DNase I (Worthington). The tube was shaken horizontally at 37℃ for 60 min at 150 rpm. Tissue suspension was passed through a 40 μm strainer, and the remaining intestine fragments were mechanically disaggregated using a syringe plunger. Cell suspensions were collected and purified by density gradient centrifugation with 30% Percoll. Intestinal DCs ($F4/80^{-}CD11c^{+}$) and macrophages ($F4/80^{+}$) were obtained from LPLs by cell sorting.

Flow cytometry and antibodies (Abs)

The following Abs were used: anti-CD11c (APC, N418), anti-F4/80 (PE, BM8), anti-gp38 (PE, 8.1.1), anti-CD31 (MEC13.3), anti-CD3ε (PE, 2C11), anti-TCRβ (APC, H57-597), anti-TCRγδ (PE/Cy7, GL3), anti-CD4 (APC-eFluor 780, RM4-5), anti-CD8α (eFluor 450, 53-6.7), anti-CD8β (FITC, eBioH35-17.2), anti-CD25 (PE, PC61.5), anti-CD5 (FITC, 53-7.3), anti-CD122 (biotin, 5H4), anti-NK1.1 (APC, PK136), anti-EpCAM (FITC, G8.8), anti-Fas (PE, SA367H8), anti-human-Bcl2 (PE, 100), anti-granzyme B (APC, NGZB), anti-PD-1 (APC, 29F.1A12), anti-IFN-γ (FITC, XMG1.2), anti-Ki67 (PE, S01A15) and rat IgG_{2b} isotype control (RTK4530). The Abs are purchased from BioLegend (San Diego, CA),

eBioscience (San Diego, CA), and TONBO Bioscience (San Diego, CA). Cells were analyzed by a FACS Verse flow cytometer (BD, Bioscience) and analyzed with FlowJo software (Tree Star, Ashland, OR).

Intracellular staining

For staining of Bcl-2, cells were fixed and permeabilized with the Foxp3/Transcription Factor Staining Buffer Set (eBioscience). PE-labeled hamster anti-mouse Bcl-2 set was used according to the manufacturer's instructions (BD Biosciences, San Jose, CA).

Immunofluorescence

Isolated section of small intestine or colon was embedded in Optimal Cutting Temperature compound (Sakura Finetechnical, Tokyo, Japan) and sliced with cryomicrotome (Leica CM3050 S, Wetzlar, Germany). Fixed samples were stained with DAPI, PE-EpCAM, FITC-CD8α or FITC-TCRγδ Abs and then mounted using PermaFluor Aqueous Mounting Medium (Thermo Fisher Scientific, Waltham, MA) and examined by a confocal laser scanning microscope (Leica TCS SP8, Wetzlar, Germany).

Real-time PCR

Total RNA was extracted with Sepasol reagent (Nacalai Tesque, Kyoto, Japan) and reverse transcribed using ReverTra Ace (Toyobo, Osaka, Japan) with random primer. cDNA was amplified in duplicate with the QuantiTect SYBR Green PCR Kit (Qiagen, Hilden, Germany) with ROX reference dye (Invitrogen) by StepOnePlus Real-Time PCR System (Thermo Fisher Scientific, Waltham, MA). PCR was undertaken at 95 ℃ for 15 sec, followed by 40 cycles consisting of 95 ℃ for 20 sec, 55 ℃ for 30 sec, and 72 ℃ for 60 sec. cDNA from splenocytes of wild type mice served as an amplification standard. Primer sequences are as

follows: granzyme B (F: 5'-TTTGTGCTGACTGCTGCTCA-3', R: 5'-TCTAGTCCTCTTGGCCTTAC-3'); IL-15 (F: 5'-AGGTCTCCCTAAAACAGAGG-3', R: 5'-GTGTATAAAGTGGTGTCAAT-3'); HPRT (F: 5'-GTTGGATACAGGCCAGACTTTGTTG-3', R: 5'-GATTCAACTTGCGCTCATCTTAGGC-3').

Dextran sodium sulfate (DSS)-induced colitis

Experimental colitis was induced by treating 12-week-old male mice with 2.5% DSS (MW 36~50 kDa, MP Biomedicals) in drinking water for 6 days, followed by a 48 hr recovery period with regular drinking water. Body weights were measured and the development of diarrhea and rectal bleeding were monitored every day. At the end of treatment, colon sections were embedded after measuring the colon length. The degree of colonic injury was assessed by a previously reported histology scoring system (24).

Fecal microbiota

Bacterial DNA was extracted from fecal samples as previously described (25). The V4 region of 16S rRNA gene was amplified by PCR with dual indexed primers as described previously (26). PCR products were purified using AMPure XP (Backman Coulter) and quantified using the Quant-iT PicoGreen ds DNA Assay Kit (Thermo Fisher Scientific). The pooled samples were sequenced on a MiSeq platform (Ilumina) with 2 × 250 bp paired-end reads. The demultiplexed data were processed with Mothur (v.1.36.1) (27) following the mothur MiSeq SOP (26). After filtering out low abundant operational taxonomic units, the data were rarefied to 30,000 reads per sample. Calculation of alpha and beta diversity and Adonis test (1,000 permutations) were performed in QIIME (v.1.8.0) (28) and the R package vegan (v.2.4.4).

Results

IELs of small and large intestines are reduced in Vil-Cre IL-15cKO mice

IL-15 is produced by IECs, macrophages, DCs and BECs in the intestine by immunohistochemistry (1). We detected IL-15 mRNA expression in each cell type by quantitative RT-PCR, and found that IECs expressed significant higher level of IL-15 than macrophages, DCs or BECs in intestine (Fig. 1A), indicating IECs are the major source of IL-15 in intestine. To investigate the function of IEC-derived IL-15 in vivo, we established IL-15-floxed mice and crossed with Vil-Cre Tg mice to obtain mice deficient in IL-15 in intestinal epithelial cells. We confirmed that IL-15 is efficiently deleted from IECs in Vil-Cre IL-15cKO mice by comparing IL-15 mRNA levels between control and Vil-Cre IL-15cKO mice (Fig. 1B). As IL-15$^{-/-}$ mice exhibited markedly reduced numbers of IELs (6), we asked whether IEC-derived IL-15 supports these cells. The cell numbers of IELs in small intestine and colon were significantly reduced in Vil-Cre IL-15cKO mice as compared with control mice, whereas thymocyte numbers were unchanged in Vil-Cre IL-15cKO mice (Fig. 1C). IELPs are reportedly defined as TCRβ^{+}CD5^{+}CD25^{-}CD4^{-}CD8α^{-}CD122^{+} (29). We detected IELPs in thymus by flow cytometry and found that the percentage and cell number of IELPs were unchanged in Vil-Cre IL-15cKO mice (Fig. 1D, 1E). These results suggest that IL-15 deletion from IEC specifically affects the maintenance of intestinal IELs without influencing IELPs.

Unconventional CD8αα IELs were reduced in Vil-Cre IL-15cKO mice

To further determine the function of IEC-derived IL-15 on IELs, we analyzed the subpopulations of IELs in Vil-Cre IL-15cKO mice. More than 90% of IELs are T cells. The percentage of TCR$\gamma\delta^{+}$ cells was lower in Vil-Cre IL-15cKO mice compared with control

mice (Fig. 2A). The ratio of $CD8\alpha^+TCR\gamma\delta^+$ IELs, most of which are $CD8\alpha\alpha^+$ TCRγδ cells, was also reduced. $TCR\alpha\beta^+$ IELs are a heterogeneous population including $CD4^+$, $CD8\alpha^+$ and $CD4^+CD8\alpha^+$ double positive (DP) cells. $CD8\alpha\alpha^+TCR\alpha\beta^+$ cells were severely impaired in Vil-Cre IL-15cKO mice. Absolute numbers of $CD8\alpha\alpha^+TCR\gamma\delta^+$ and $CD8\alpha\alpha^+TCR\alpha\beta^+$ cells, known as unconventional IELs in small intestine, were dramatically reduced in Vil-Cre IL-15cKO mice (Fig. 2B). In contrast, numbers of $CD4^+TCR\alpha\beta^+$ and $CD8\alpha\beta^+TCR\alpha\beta^+$ cells were unchanged. Similar results were observed in the colonic IELs (Fig. 2C).

Besides T cells, $CD3^-NK1.1^+$ NK cells in IELs were also significantly reduced in Vil-Cre IL-15cKO mice (Fig. 2B). CD8αα T cells reside in lamina propria as well. We found that $CD8\alpha\alpha^+TCR\gamma\delta^+$ and $CD8\alpha\alpha^+TCR\alpha\beta^+$ cells were reduced in lamina propria of Vil-Cre IL-15cKO mice (Fig. 2D). Because NK cells in lamina propria were reported to be reduced in $IL\text{-}15^{-/-}$ mice (30), we analyzed NK cells in lamina propria as $CD3^-NK1.1^+CD27^+CD127^-$ cells. We found that instead of IEC-derived IL-15, their maintenance is dependent on hematopoietic cell- or BEC-derived IL-15 (Fig. 2D, Fig. S1). The decrease of $CD8\alpha^+$ and $TCR\gamma\delta^+$ IELs was also confirmed in small intestine of Vil-Cre IL-15cKO mice by immunohistochemistry (Fig. 2E). Taken together, these results indicate that IEC-derived IL-15 plays a critical and selective role for maintenance of IELs in the intestine.

IEL subsets are unchanged in Tie2-Cre IL-15cKO mice

Previously report showed that IL-15 is produced not only by IEC but also by BEC and hematopoietic cells such as macrophages and dendritic cells in the intestine (1). To study whether BEC- or hematopoietic cell-derived IL-15 maintains IELs, we analyzed Tie2-Cre IL-15cKO mice. IL-15 mRNA expression in BECs was significantly lower in Tie2-Cre IL-15cKO mice than in control mice (Fig. 3A). We found the ratio of $CD8\alpha^+TCR\gamma\delta^+$, $CD8\alpha\alpha^+TCR\alpha\beta^+$ and $CD8\alpha\beta^+TCR\alpha\beta^+$ IELs were unchanged in Tie2-Cre IL-15cKO mice

compared with control mice (Fig. 3B). Absolute numbers of total IELs, as well as CD8αα^{+}TCRγδ^{+} and CD8αα^{+}TCRαβ^{+} IELs were also unchanged (Fig. 3C). These results suggest that BEC- or hematopoietic cell-derived IL-15 is dispensable for the maintenance of CD8αα IELs.

Cell survival is impaired in CD8αα IELs in Vil-Cre IL-15cKO mice

To elucidate the mechanisms involved in reduction of CD8αα IELs, we stained freshly isolated IELs with the apoptotic marker Annexin V and propidium iodide (PI) to assess cell apoptosis. Frequency of early apoptotic (Annexin V^{+}, PI^{-}) and dead (Annexin V^{+}, PI^{+}) cells were higher in CD8αα^{+}TCRαβ^{+} and CD8αα^{+}TCRγδ^{+} IELs of Vil-Cre IL-15cKO mice (Fig. 4A, B), indicating that apoptosis of CD8αα IELs was enhanced in Vil-Cre IL-15cKO mice. IL-15 promotes survival of CD8αα IELs by inducing anti-apoptotic proteins, such as Bcl-2 (9). To determine whether IEC-derived IL-15 alters expression of Bcl-2 in CD8αα IELs, we analyzed expression of Bcl-2 protein by intracellular staining and flow cytometry. Bcl-2 expression was reduced in CD8αα^{+}TCRαβ^{+} and CD8αα^{+}TCRγδ^{+} IELs of Vil-Cre IL-15cKO mice. CD4^{+}TCRαβ^{+} and CD8αβ^{+}TCRαβ^{+} IELs also showed slightly reduced Bcl-2 expression in Vil-Cre IL-15cKO mice, nevertheless their cell numbers were unchanged (Fig. 4C).

Fas-mediated apoptosis is an important pathway promoting cell death in activated T cells (31). Because the susceptibility of CD8αα IELs to undergo apoptosis is increased in Vil-Cre IL-15cKO mice, as indicated by the reduced Bcl-2 expression, we then analyzed Fas expression of CD8αα IELs. We found that Fas expression was slightly higher in CD8αα^{+}TCRαβ^{+} and CD8αα^{+}TCRγδ^{+} IELs of Vil-Cre IL-15cKO mice than those of control mice. As a comparison, Fas expression of CD4^{+}TCRαβ^{+} and CD8αβ^{+}TCRαβ^{+} IELs was

similar in control and Vil-Cre IL-15cKO mice (Fig. 4D). This result further suggested that CD8αα IELs in Vil-Cre IL-15cKO mice are apt to go through Fas-mediated apoptosis. CD122$^{-/-}$ mice exhibited a dramatic reduction in CD8αα IELs as well as IL-15$^{-/-}$ mice (7), suggesting a significant role of CD122 in IELs maintenance. We observed that CD122 expression was reduced in CD8αα IELs but not in conventional IELs of Vil-Cre IL-15cKO mice (Fig. 4E, F). These results indicate that IEC-derived IL-15 is required for survival of CD8αα IELs.

IELs were partially restored in Bcl-2Tg × Vil-Cre IL-15cKO mice.

To test whether survival signal via Bcl-2 is involved in IL-15-mediated homeostasis of CD8αα IELs, we introduced a Bcl-2 transgene into Vil-Cre IL-15cKO mice. Bcl-2 was expressed in CD8αα IELs in Bcl-2Tg × Vil-Cre IL-15cKO (Bcl-2 Vil-Cre IL-15cKO) mice other than control and Vil-Cre IL-15cKO mice when detected with anti-human Bcl-2 Ab (Fig. 5A). The percentage of TCRγδ^{+} cells in Bcl-2Tg × Vil-Cre IL-15cKO (Bcl-2 Vil-Cre IL-15cKO) mice was comparable to that of Vil-Cre IL-15cKO mice, whereas the percentage of CD8αα^{+}TCRαβ^{+} cells was increased in Bcl-2 Vil-Cre IL-15cKO mice (Fig. 5B). Absolute numbers of CD8αα^{+}TCRαβ^{+} and CD8αα^{+}TCRγδ^{+} IELs were significantly increased in Bcl-2 Vil-Cre IL-15cKO mice by enforced expression of Bcl-2. However, they were still lower than those of IL-15$^{f/f}$ control mice (Fig. 5C), suggesting that CD8αα IELs in Vil-Cre IL-15cKO mice were partially restored by the Bcl-2 transgene. CD4^{+}TCRαβ^{+} T cells were comparable in three types of mice, whereas the Bcl-2 transgene significantly increased the cell number of CD8αβ^{+}TCRαβ^{+} cells (Fig. 5C). CD8αα^{+}TCRαβ^{+} and CD8αα^{+}TCRγδ^{+} LPLs were also increased in Bcl-2 Vil-Cre IL-15cKO mice, and no significant difference of NK cells was found between Bcl-2 Vil-Cre IL-15cKO mice and Vil-Cre IL-15cKO mice (Fig.

5D). As the apoptosis of CD8αα IELs was enhanced in Vil-Cre IL-15cKO mice, we asked whether apoptosis was reduced by the Bcl-2 transgene. We stained IELs with annexin V and PI, and found that annexin $V^+PI^-CD8\alpha\alpha^+TCR\gamma\delta^+$ IELs in Bcl-2 Vil-Cre IL-15cKO mice were reduced to the similar level of that in control mice. However, cell number of annexin $V^+PI^-CD8\alpha\alpha^+TCR\alpha\beta^+$ IELs in Bcl-2 Vil-Cre IL-15cKO mice was unchanged compared to that in Vil-Cre IL-15cKO mice (Fig. 5E, 5F).

We also analyzed the expression of Fas and CD122 on CD8αα IELs in Bcl-2 Vil-Cre IL-15cKO and Vil-Cre IL-15cKO mice. Even though $CD8\alpha\alpha^+TCR\gamma\delta^+$ IELs displayed comparable levels of Fas expression in Vil-Cre IL-15cKO and $IL\text{-}15^{f/f}$ control mice, $CD8\alpha\alpha^+TCR\alpha\beta^+$ IELs showed lower level of Fas expression in Bcl-2 Vil-Cre IL-15cKO mice than in Vil-Cre IL-15cKO mice (Fig. 5G). Similar with Fas expression, CD122 expression of $CD8\alpha\alpha^+TCR\gamma\delta^+$ IELs is comparable in Bcl-2 Vil-Cre IL-15cKO and Vil-Cre IL-15cKO mice, while CD122 expression of $CD8\alpha\alpha^+TCR\alpha\beta^+$ IELs is lower in Bcl-2 Vil-Cre IL-15cKO mice than Vil-Cre IL-15cKO mice (Fig. 5H). These results suggested that although an enforced expression of Bcl-2 restores the number of CD8αα IELs in IL-15cKO mice, it is not sufficient to generate phenotypically equivalent CD8αα IELs.

IEC-derived IL-15 promotes granzyme B expression in CD8αα IELs.

Although a specific function for CD8αα IELs has not been described yet, they have a potent antigen-experienced cytotoxic effector phenotype, characterized by high levels of granzyme expression (3). We detected significantly lower levels of granzyme B expression in $CD8\alpha\alpha^+TCR\alpha\beta^+$ and $CD8\alpha\alpha^+TCR\gamma\delta^+$ IELs of Vil-Cre IL-15cKO mice compared with control mice (Fig. 6A, 6B). Reduced levels of granzyme B transcripts were confirmed in $CD8\alpha\alpha^+TCR\alpha\beta^+$ Vil-Cre IL-15cKO mice by RT-qPCR (Fig. 6C). These results suggested

that IEC-derived IL-15 is important for granzyme B production in CD8αα IELs to promote their functional maturation. Furthermore, we found that PD-1 expression of CD8αα IELs was elevated in Vil-Cre IL-15cKO mice (Fig. 6D, 6E). Most of CD8αα IELs were PD-1^{-}. We found that PD-1^{+}CD8αα IELs exist in a small amount and that they were negative for granzyme B expression. PD-1^{+}GzmB^{-} CD8αα γδIELs and αβIELs were unchanged in Vil-Cre IL-15cKO mice, while PD-1^{-}GzmB^{-} and PD-1^{-}GzmB^{+} were reduced (Fig. 6F, 6G), suggesting that the PD-1^{-} mature subpopulation in CD8αα IEL is indispensably dependent on IEC-derived IL-15.

DSS-induced colitis is unchanged in Vil-Cre IL-15cKO mice

IL-15 is involved in the pathogenesis of colitis. It is reported that DSS-induced colitis is alleviated in IL-15$^{-/-}$ mice (32). Additionally, overexpression of human IL-15 in intestinal epithelial cells of mice induces chronic inflammation in small intestine (33). However, the precise role of IEC-derived IL-15 in colitis is not understood yet. To address this question, we first analyzed the fecal microbiota composition and found no significant differences in alpha and beta diversity between control and Vil-Cre IL-15cKO mice (Fig. S2). Then, we induced acute colitis in mice by treating with 2.5% DSS in drinking water. Body weight loss, feces score, and colon length were unchanged in DSS-treated Vil-Cre IL-15cKO mice compared to control mice (Fig. S3A-S3C). Vil-Cre IL-15cKO mice might have showed slightly severer lesion judging from their higher histological scores than control mice at recovering phase on day 7, although there was no statistical significance (Fig. S3D-S3F). IL-15 production by colonic IEC was reduced after DSS treatment, and Vil-Cre IL-15 showed a deficiency of IL-15 production in IECs (Fig. S3G). IFN-γ–producing Th1 cells and NK cells were unchanged between control and Vil-Cre IL-15cKO mice after DSS treatment (Fig. S3H, S3I). Collectively, these data suggested that DSS-induced colitis was not

alleviated in Vil-Cre IL-15cKO mice in comparison with control mice, implying that IEC-derived IL-15 does not play a major role in induction of and recovery from colitis.

Discussion

In this study, we determined local functions of intestinal IL-15 in development and maintenance of IELs using IL-15-floxed and Vil-Cre or Tie2-Cre mice. Abnormal IEL profiles have been reported in IL-15$^{-/-}$, IL-15Rα$^{-/-}$, and IL-2Rβ$^{-/-}$ mice. Because IL-15 is expressed by different cell types in tissues, the cells producing IL-15 vital for IELs remain unclear. Recently, it is reported that Vil-Cre IL-15Rα$^{f/f}$ mice show similar reduction of IELs, indicating that the IL-15Rα of IECs is important for IEL maintenance. Vil-Cre IL-15cKO mice showed similar deficiency of IELs, in which CD8αα IELs were selectively reduced. By contrast, CD8αα IELs were unchanged in Tie2-Cre IL-15cKO mice, in which IL-15 production is deleted from endothelial cells, DCs and macrophages. These results suggested that the maintenance of CD8αα IELs totally depends on IL-15 produced by IECs.

We found that small intestinal and colonic IELs were reduced in Vil-Cre IL-15cKO mice, whereas IELPs were unchanged in thymus, suggesting that IEC-derived IL-15 play a local role on IELs. Furthermore, only CD8αα IELs were significantly reduced, whereas CD4^{+}TCRαβ^{+} and CD8αβ^{+}TCRαβ^{+} IELs were unchanged. It is consistent with the commonly accepted view that CD4^{+}TCRαβ^{+} and CD8αβ^{+}TCRαβ^{+} IELs do not depend on IEC-derived IL-15 despite their expression of CD122 (34). They might rely on other factors such as IL-7 in intestines. Bcl-2 expression in CD8αα IELs was reduced in Vil-Cre IL-15cKO mice, and overexpression of Bcl-2 only partially rescued CD8αα IELs. In addition, we observed that granzyme B expression was reduced, whereas PD-1 expression was increased. These results demonstrate that IEC-derived IL-15 plays an indispensable role in maintenance and maturation of CD8αα IELs. Thus, our study suggests that IECs provide a unique IL-15 niche for CD8αα IELs. In addition, since both IEC-derived IL-15Rα and IL-15

play similarly critical roles in CD8αα IELs, it is suggested that IEC promotes the maintenance of CD8αα IELs through trans-presentation of IL-15 to CD8αα IELs.

IL-15 promotes the survival of CD8αα IELs through up-regulating Bcl-2. It is reported that enforced expression of Bcl-2 partially restores TCRγδ^{+} IELs (35). Here we found that overexpression of Bcl-2 partially recovered both CD8αα^{+}TCRαβ^{+} and CD8αα^{+}TCRγδ^{+} IELs in Vil-Cre IL-15cKO mice, but not to the normal level of control mice. These results indicate that besides Bcl-2, other IL-15 signal is required for maintaining CD8αα IELs. It is suggested that IL-15 promotes survival of CD8αα IELs not only by inducing Bcl-2 expression but also by facilitating the dissociation of Bim from Bcl-2 and that deletion of Bim from CD8αα IELs increased their survival in IL-15Rα$^{-/-}$ mice (9). There are two different subpopulations, CD122^{high} and CD122^{low}, in CD8αα IELs. We speculate that CD122^{high} CD8αα IELs might be generated and maintained from CD122^{low} CD8αα IELs via IL-15 signal. This hypothesis is supported by the result that CD8αα IELs in Vil-Cre IL-15cKO mice, most of which are CD122^{low}, are actively proliferating (Fig. S3A, B). Another support is that CD8αα^{+}TCRαβ^{+} IELs in Bcl-2 Vil-Cre IL-15cKO mice showed lower CD122 expression, suggesting that the overexpression of Bcl-2 can increase the CD122^{low} subset. The CD122^{low} CD8αα IELs failed to adequately respond to IL-15, which probably promoted its deficiency. TCRγδ^{+} IELs might also be reduced because of failed residency in epithelium, which is supported by IEC-derived IL-15 (36).

We also found increased Fas expression in CD8αα IELs of Vil-Cre IL-15cKO mice. It is reported that IL-15 efficiently inhibits apoptosis induced by anti-Fas antibodies (37). In addition, IL-15 can rescue CD7^{-}CD4^{+} memory T cells, a cell type with higher apoptosis rate, by down-regulating Fas expression (38). Similarly, we found that Fas expression and Annexin V staining was increased in CD8αα IELs of Vil-Cre IL-15cKO mice, suggesting

that IL-15 might promote the survival of CD8αα IELs by down-regulating Fas expression. The relationship between IL-15 and Fas signaling pathways is still unclear. Because the cooperation between STAT3 and c-Jun reduces Fas transcription (39), IL-15 might suppress Fas expression by activating STAT3 pathway.

IL-15 is a cytokine critical for survival and function of NK cells (40,41). Our results showed that IEC-derived IL-15 maintains NK cells in IELs. CD8αα IELs are considered as NK-like cells, because they express various NK receptors such as Ly49E and 2B4 (2). Thus, they might receive similar IL-15 signals as NK cells. We found that IL-15 promotes not only survival but also functional maturation of CD8αα IELs by inducing granzyme B expression. It is recently reported that T-bet, through interacting with XBP1s, a transcription factor stabilized by IL-15 signaling, promotes granzyme B production in NK cells (42). Because T-bet regulates development and functional maturation of IELs (12,43), thus T-bet might regulate granzyme B production in CD8αα IELs by IL-15 signals like it does in NK cells.

As IELPs express high levels of PD-1, while matured CD8αα IELs are PD-1^{low}, PD-1 is down-regulated during maturation of CD8αα IELs. CD8αα IELs in Vil-Cre IL-15cKO mice showed higher level of PD-1 expression, suggesting that IEC-derived IL-15 might play some role in down-regulating PD-1 during their maturation. PD-1^{+} CD8αα IELs are found to be granzyme B^{+}, which reflected their immature character. PD-1^{+}GzmB^{-}CD8αα IELs is unaffected by the deficiency of IEC-derived IL-15, whereas PD-1^{-}GzmB^{-} is mildly and PD-1^{-}GzmB^{+} is severely affected. Thus, we suspect that CD8αα IEL precursors might go through a process as first down-regulating their PD-1 expression and then producing granzyme B with the function of IEC-produced IL-15 in intestine. Alternatively, increased PD-1 on lymphocyte might be a symbol of cell exhaustion, which is accompanied by reduced effector functions. We found the increased apoptosis and reduced granzyme B production in

CD8αα IELs of Vil-Cre IL-15cKO mice. These results might suggest that IEC-derived IL-15 prevents CD8αα IELs from exhaustion after continuous activation by microbiota.

Although DSS-induced colitis is alleviated in IL-15$^{-/-}$ mice compared to control mice (23), the pathology of colitis is only slightly aggravated in Vil-Cre IL-15cKO mice, suggesting that IL-15 produced by other cells might play a detrimental role in the progression of colitis. Further studies are needed to clarify the role of each cell type-derived IL-15 on colitis. In addition, how CD8αα IELs functions in colitis is unclear. AhR$^{-/-}$ mice, in which unconventional IELs were significantly reduced, exhibited increased severity of colitis than control mice (44). Consistently, TCRγδ lymphocyte-deficient mice showed increased susceptibility to colitis (45). Both studies emphasized the importance of IELs in reducing DSS-induced colitis. In our study, severe reduction of CD8αα IELs is not accompanied by severer pathology of colitis in Vil-Cre IL-15cKO mice, suggesting that besides IELs, other factors might function synergistically to influence the progression of colitis.

In summary, we defined the role of IL-15 produced by intestinal epithelial cells in maintenance and maturation of IELs using IEC-specific IL-15 conditional knockout mice. We showed that IEC-derived IL-15 maintains the survival of unconventional IELs by up-regulating Bcl-2 and down-regulating Fas expression. IL-15 signal maintains CD122 expression and granzyme B production. Especially, we found that IEC-derived IL-15 might suppress PD-1 expression on IELs. Our results indicated a new developmental pathway from immature CD8αα IELs with low expression of Bcl-2, CD122, and granzyme B, and high expression of Fas and PD-1, into mature CD8αα IELs with high expression of Bcl-2, CD122, and granzyme B, and low expression of Fas and PD-1. The development from the immature to the mature stages depends on IEC-derived IL-15. Thus, our study provides new insights on functions of IEC-derived IL-15 on IELs.

Funding

This work was supported by JSPS KAKENHI Grant Numbers 16K15288, 16H05172, and 15H01153 (K.I.), 17K15721 (G.C.), 26460572 (S.T.), and 16K08835 (T.H.); and by the Joint Usage/Research Center program of Institute for Frontier Life and Medical Sciences Kyoto University.

Acknowledgments

We would like to acknowledge Dr. R. Kageyama for local supply of the Vil-Cre Tg mice; Dr. J. Domen for the H2K-Bcl-2 transgenic mice; Mr. H. Miyachi and Ms. S. Kitano for manipulating mouse embryos; and members of the K. Ikuta laboratory for discussion.

References

1 Cui, G., Hara, T., Simmons, S., Wagatsuma, K., Abe, A., Miyachi, H., Kitano, S., Ishii, M., Tani-Ichi, S., and Ikuta, K. 2014. Characterization of the IL-15 niche in primary and secondary lymphoid organs in vivo. *Proc. Natl. Acad. Sci. USA.* 111:1915.

2 Denning, T. L., Granger, S., Mucida, D., Graddy, R., Leclercq, G., Zhang, W., Honey, K., Rasmussen, J. P., Cheroutre, H., and Rudensky, A. Y. 2007. Mouse TCRαβ^{+}CD8αα intraepithelial lymphocytes express genes that down-regulate their antigen reactivity and suppress immune responses. *J. Immunol.* 178:4230.

3 Shires, J. 2004. Biological insights into intraepithelial lymphocytes provided by serial analysis of gene expression. *Immunity* 15:419.

4 Boismenu, R. and Havran, W. L. 1994. Modulation of epithelial cell growth by intraepithelial γδ T cells. *Science* 266:1253.

5 Lodolce, J. P., Boone, D. L., Chai, S., Swain, R. E., Dassopoulos, T., Trettin, S., and Ma, A. 1998. IL-15 receptor maintains lymphoid homeostasis by supporting lymphocyte homing and proliferation. *Immunity* 9:669.

6 Kennedy, M. K., Glaccum, M., Brown, S. N., Butz, E. A., Viney, J. L., Embers, M., Matsuki, N., Charrier, K., Sedger, L., and Willis, C. R. 2000. Reversible defects in natural killer and memory CD8 T cell lineages in interleukin 15–deficient mice. *J. Exp. Med.* 191:771.

7 Suzuki, H., Duncan, G. S., Takimoto, H., and Mak, T. W. 1997. Abnormal development of intestinal intraepithelial lymphocytes and peripheral natural killer cells in mice lacking the IL-2 receptor β chain. *J. Exp. Med.* 185:499.

8 Ma, L. J., Acero, L. F., Zal, T., and Schluns, K. S. 2009. Trans-presentation of IL-15 by intestinal epithelial cells drives development of CD8αα IELs. *J. Immunol.*

183:1044.

9 Lai, Y. G., Hou, M. S., Lo, A., Huang, S. T., Huang, Y. W., Yang-Yen, H. F., and Liao, N. S. 2013. IL-15 modulates the balance between Bcl-2 and Bim via a Jak3/1-PI3K-Akt-ERK pathway to promote CD8αα$^+$ intestinal intraepithelial lymphocyte survival. *Eur. J. Immunol.* 43:2305.

10 Lai, Y.-G., Hou, M.-S., Hsu, Y.-W., Chang, C.-L., Liou, Y.-H., Tsai, M.-H., Lee, F., and Liao, N.-S. 2008. IL-15 does not affect IEL development in the thymus but regulates homeostasis of putative precursors and mature CD8αα$^+$ IELs in the intestine. *J. Immunol.* 180:3757.

11 Chu, C.-L., Chen, S.-S., Wu, T.-S., Kuo, S.-C., and Liao, N.-S. 1999. Differential effects of IL-2 and IL-15 on the death and survival of activated TCRγδ$^+$ intestinal intraepithelial lymphocytes. *J. Immunol.* 162:1896.

12 Klose, C. S., Blatz, K., d'Hargues, Y., Hernandez, P. P., Kofoed-Nielsen, M., Ripka, J. F., Ebert, K., Arnold, S. J., Diefenbach, A., and Palmer, E. 2014. The transcription factor T-bet is induced by IL-15 and thymic agonist selection and controls CD8αα$^+$ intraepithelial lymphocyte development. *Immunity* 41:230.

13 Zhao, H., Nguyen, H., and Kang, J. 2005. Interleukin 15 controls the generation of the restricted T cell receptor repertoire of γδ intestinal intraepithelial lymphocytes. *Nat. Immunol.* 6:1263.

14 Schluns, K. S., Nowak, E. C., Cabrera-Hernandez, A., Puddington, L., Lefrançois, L., and Aguila, H. L. 2004. Distinct cell types control lymphoid subset development by means of IL-15 and IL-15 receptor α expression. *Proc. Natl. Acad. Sci. USA.* 101:5616.

15 Mortier, E., Advincula, R., Kim, L., Chmura, S., Barrera, J., Reizis, B., Malynn, B. A., and Ma, A. 2009. Macrophage- and dendritic-cell-derived interleukin-15 receptor

alpha supports homeostasis of distinct $CD8^+$ T cell subsets. *Immunity* 31:811.

16 Cooper, M. A., Bush, J. E., Fehniger, T. A., VanDeusen, J. B., Waite, R. E., Liu, Y., Aguila, H. L., and Caligiuri, M. A. 2002. In vivo evidence for a dependence on interleukin 15 for survival of natural killer cells. *Blood* 100:3633.

17 Marçais, A., Cherfils-Vicini, J., Viant, C., Degouve, S., Viel, S., Fenis, A., Rabilloud, J., Mayol, K., Tavares, A., and Bienvenu, J. 2014. The metabolic checkpoint kinase mTOR is essential for IL-15 signaling during the development and activation of NK cells. *Nature immunology* 15:749.

18 El Marjou, F., Janssen, K. P., Hung-Junn Chang, B., Li, M., Hindie, V., Chan, L., Louvard, D., Chambon, P., Metzger, D., and Robine, S. 2004. Tissue-specific and inducible Cre-mediated recombination in the gut epithelium. *Genesis* 39:186.

19 Domen, J., Gandy, K. L., and Weissman, I. L. 1998. Systemic overexpression of BCL-2 in the hematopoietic system protects transgenic mice from the consequences of lethal irradiation. *Blood* 91:2272.

20 Hase, K., Ohshima, S., Kawano, K., Hashimoto, N., Matsumoto, K., Saito, H., and Ohno, H. 2005. Distinct gene expression profiles characterize cellular phenotypes of follicle-associated epithelium and M cells. *DNA Research* 12:127.

21 Stzepourginski, I., Eberl, G., and Peduto, L. 2015. An optimized protocol for isolating lymphoid stromal cells from the intestinal lamina propria. *J. Immunol. Methods* 421:14.

22 Ishikawa, H., Li, Y., Abeliovich, A., Yamamoto, S., Kaufmann, S., and Tonegawa, S. 1993. Cytotoxic and interferon γ-producing activities of γδ T cells in the mouse intestinal epithelium are strain dependent. *Proc. Natl. Acad. Sci. USA.* 90:8204.

23 Hadis, U., Wahl, B., Schulz, O., Hardtke-Wolenski, M., Schippers, A., Wagner, N., Müller, W., Sparwasser, T., Förster, R., and Pabst, O. 2011. Intestinal tolerance

requires gut homing and expansion of FoxP3$^+$ regulatory T cells in the lamina propria. *Immunity* 34:237.

24 Liu, S., Qian, Y., Li, L., Wei, G., Guan, Y., Pan, H., Guan, X., Zhang, L., Lu, X., and Zhao, Y. 2013. Lgr4 gene deficiency increases susceptibility and severity of dextran sodium sulfate-induced inflammatory bowel disease in mice. *J. Biol. Chem.* 288:8794.

25 Okai, S., Usui, F., Yokota, S., Hori-i, Y., Hasegawa, M., Nakamura, T., Kurosawa, M., Okada, S., Yamamoto, K., and Nishiyama, E. 2016. High-affinity monoclonal IgA regulates gut microbiota and prevents colitis in mice. *Nat. Microbiol.* 1:16103.

26 Kozich, J. J., Westcott, S. L., Baxter, N. T., Highlander, S. K., and Schloss, P. D. 2013. Development of a dual-index sequencing strategy and curation pipeline for analyzing amplicon sequence data on the MiSeq Illumina sequencing platform. *Appl. Environ. Microbiol.* 79:5112.

27 Schloss, P. D., Westcott, S. L., Ryabin, T., Hall, J. R., Hartmann, M., Hollister, E. B., Lesniewski, R. A., Oakley, B. B., Parks, D. H., and Robinson, C. J. 2009. Introducing mothur: open-source, platform-independent, community-supported software for describing and comparing microbial communities. *Appl. Environ. Microbiol.* 75:7537.

28 Caporaso, J. G., Kuczynski, J., Stombaugh, J., Bittinger, K., Bushman, F. D., Costello, E. K., Fierer, N., Pena, A. G., Goodrich, J. K., and Gordon, J. I. 2010. QIIME allows analysis of high-throughput community sequencing data. *Nat. Methods* 7:335.

29 Ruscher, R., Kummer, R. L., Lee, Y. J., Jameson, S. C., and Hogquist, K. A. 2017. CD8αα intraepithelial lymphocytes arise from two main thymic precursors. *Nat. Immunol.* 18:771.

30 Schulthess, J., Meresse, B., Ramiro-Puig, E., Montcuquet, N., Darche, S., Bègue, B., Ruemmele, F., Combadière, C., Di Santo, J. P., and Buzoni-Gatel, D. 2012. Interleukin-15-dependent NKp46$^+$ innate lymphoid cells control intestinal

inflammation by recruiting inflammatory monocytes. *Immunity* 37:108.

31 Aggarwal, S. and Gupta, S. 1998. Increased apoptosis of T cell subsets in aging humans: altered expression of Fas (CD95), Fas ligand, Bcl-2, and Bax. *J. Immunol.* 160:1627.

32 Yoshihara, K., Yajima, T., Kubo, C., and Yoshikai, Y. 2006. Role of interleukin 15 in colitis induced by dextran sulphate sodium in mice. *Gut* 55:334.

33 Ohta, N., Hiroi, T., Kweon, M.-N., Kinoshita, N., Jang, M. H., Mashimo, T., Miyazaki, J.-I., and Kiyono, H. 2002. IL-15-dependent activation-induced cell death-resistant Th1 type CD8αβ^{+}NK1.1^{+} T cells for the development of small intestinal inflammation. *J. Immunol.* 169:460.

34 Qiu, Y., Wang, W., Xiao, W., and Yang, H. 2015. Role of the intestinal cytokine microenvironment in shaping the intraepithelial lymphocyte repertoire. *J. Leukoc. Biol.* 97:849.

35 Nakazato, K., Yamada, H., Yajima, T., Kagimoto, Y., Kuwano, H., and Yoshikai, Y. 2007. Enforced expression of Bcl-2 partially restores cell numbers but not functions of TCRγδ intestinal intraepithelial T lymphocytes in IL-15-deficient mice. *J. Immunol.* 178:757.

36 Hu, M. D., Ethridge, A. D., Lipstein, R., Kumar, S., Wang, Y., Jabri, B., Turner, J. R., and Edelblum, K. L. 2018. Epithelial IL-15 is a critical regulator of γδ intraepithelial lymphocyte motility within the intestinal mucosa. *J. Immunol.* 201:747.

37 Bulfone-Paus, S., Ungureanu, D., Pohl, T., Lindner, G., Paus, R., Rückert, R., Krause, H., and Kunzendorf, U. 1997. Interleukin-15 protects from lethal apoptosis *in vivo*. *Nat. Med.* 3:1124.

38 Rappl, G., Abken, H., Hasselmann, D., Tilgen, W., Ugurel, S., and Reinhold, U. 2001. The CD7^{-} subset of CD4^{+} memory T cells is prone to accelerated apoptosis that is

prevented by interleukin-15 (IL-15). *Cell Death Differ.* 8:395.

39 Ivanov, V. N., Krasilnikov, M., and Ronai, Z. 2002. Regulation of Fas expression by STAT3 and c-Jun is mediated by phosphatidylinositol 3-kinase-AKT signaling. *J. Biol. Chem.* 277:4932.

40 Carson, W. E., Fehniger, T. A., Haldar, S., Eckhert, K., Lindemann, M. J., Lai, C.-F., Croce, C. M., Baumann, H., and Caligiuri, M. A. 1997. A potential role for interleukin-15 in the regulation of human natural killer cell survival. *J. Clin. Invest.* 99:937.

41 Nandagopal, N., Ali, A. K., Komal, A. K., and Lee, S.-H. 2014. The critical role of IL-15–PI3K–mTOR pathway in natural killer cell effector functions. *Front. Immunol.* 5:187.

42 Wang, Y., Zhang, Y., Yi, P., Dong, W., Nalin, A. P., Zhang, J., Zhu, Z., Chen, L., Benson, D. M., and Mundy-Bosse, B. L. 2019. The IL-15–AKT–XBP1s signaling pathway contributes to effector functions and survival in human NK cells. *Nat. Immunol.* 20:10.

43 Reis, B. S., van Konijnenburg, D. P. H., Grivennikov, S. I., and Mucida, D. 2014. Transcription factor T-bet regulates intraepithelial lymphocyte functional maturation. *Immunity* 41:244.

44 Li, Y., Innocentin, S., Withers, D. R., Roberts, N. A., Gallagher, A. R., Grigorieva, E. F., Wilhelm, C., and Veldhoen, M. 2011. Exogenous stimuli maintain intraepithelial lymphocytes via aryl hydrocarbon receptor activation. *Cell* 147:629.

45 Chen, Y., Chou, K., Fuchs, E., Havran, W. L., and Boismenu, R. 2002. Protection of the intestinal mucosa by intraepithelial γδ T cells. *Proc. Natl. Acad. Sci. USA.* 99:14338.

Figure Legends

Figure 1. Loss of IELs in Vil-Cre IL-15cKO mice.

(A) qRT-PCR analysis of IL-15 mRNA expression by IECs, macrophages, DCs and BECs. Expression levels were normalized to HPRT (n = 3). (B) IL-15 mRNA expression in IECs of control and Vil-Cre IL-15cKO mice was analyzed by qRT-PCR and normalized to those of HPRT (n = 3). (C) The numbers of small intestinal (n = 9) and colonic (n = 3) IELs and thymocytes (n=4) of control and Vil-Cre IL-15cKO mice. (D) Flow cytometry analysis of IEL precursors in the thymus of Vil-Cre IL-15cKO mice. IEL precursors were analyzed as $CD4^{-}CD8\alpha^{-}TCR\beta^{+}CD5^{+}CD25^{-}CD122^{+}$. (E) The numbers of IEL precursors in thymus of control and Vil-Cre IL-15cKO mice (n = 4). Data are means ± SEM. Student's *t*-tests for unpaired data were used to compare values between two groups. *, $p < 0.05$; n.s., not significant.

Figure 2. CD8αα IELs are selectively reduced in Vil-Cre IL-15cKO mice.

(A) IELs from the small intestine of control or Vil-Cre IL-15cKO mice were stained as indicated. The percentages of cells for a given phenotype relative to the gated population are shown. (B–C) The absolute numbers of the indicated IEL subsets in the small intestine (B) (n = 6) or colon (C) (n = 3) of individual mice were calculated. (D) The absolute numbers of the indicated LPL subsets in the small intestine (n=3). (E) Tissue samples from the small intestine of control or Vil-Cre IL-15cKO mice were stained with anti-CD8α (blue), anti-TCRγδ (green) or anti-EpCAM (red) antibody. Student's *t*-tests for unpaired data were used to compare values between two groups. *, $p < 0.05$; n.s., not significant.

Figure 3. CD8αα IELs are unchanged in Tie2-Cre IL-15cKO mice.

(A) IL-15 mRNA expression in BECs of control and Tie2-Cre IL-15cKO mice was analyzed by qRT-PCR and normalized to those of HPRT (n = 3). (B) IELs from control or Tie2-Cre IL-15cKO mice were stained as indicated. The percentages of cells for a given phenotype relative to the gated population are shown. (C) The absolute numbers of the indicated IEL subsets in the small intestine of individual mice were calculated (n = 3). Student's *t*-tests for unpaired data were used to compare values between two groups. n.s., not significant.

Figure 4. IEC-derived IL-15 is required for the homeostasis of CD8αα IELs.

(A) CD8αα^{+}TCRγδ^{+} and CD8αα^{+}TCRαβ^{+} IELs of control and Vil-Cre IL-15cKO mice were stained with annexin V and propidium iodide (PI) and analyzed by flow cytometry. (B) Percentages of Annexin V^{+} PI^{-} early apoptotic cells in CD8αα^{+}TCRγδ^{+} and CD8αα^{+}TCRαβ^{+} IELs were calculated (n = 3). Student's *t*-tests for unpaired data were used to compare values between two groups. (C–E) IELs were isolated from control or Vil-Cre IL-15cKO mice, and stained with anti-Bcl-2, anti-Fas, and anti-CD122 Abs. Representative histograms show intracellular Bcl-2 (C), Fas (D) and CD122 (E) expression of the indicated IEL subsets. Data represent one of two independent experiments with similar results. (F) Mean fluorescence intensity (MFI) of CD122 expression on CD8αα IELs of control and Vil-Cre IL-15cKO mice were calculated (n = 3). Student's *t*-tests for unpaired data were used to compare values between two groups. *, $p < 0.05$; n.s., not significant.

Figure 5. Enforced expression of Bcl-2 partially restores the number of IELs in Vil-Cre IL-15cKO mice.

(A) IELs were isolated from IL-15$^{f/f}$, Vil-Cre IL-15cKO, or Bcl-2 Vil-Cre IL-15cKO mice, and stained with anti-human Bcl-2 antibody. Representative histograms show intracellular

Bcl-2 expression of CD8αα^{+}TCRγδ^{+} and CD8αα^{+}TCRαβ^{+} IELs. Data represent one of two independent experiments with similar results. (B) IELs from Vil-Cre IL-15cKO or Bcl-2 Vil-Cre IL-15cKO mice were stained as indicated. The percentages of cells for a given phenotype relative to the gated population are shown. (C) The absolute numbers of the indicated IEL subsets in the small intestine of IL-15$^{f/f}$ control, Vil-Cre IL-15cKO mice or Bcl-2 Vil-Cre IL-15cKO mice were calculated (n = 4). (D) The absolute numbers of the indicated LPL subsets in the small intestine of control, Vil-Cre IL-15cKO, and Bcl-2 Vil-Cre IL-15cKO mice were calculated (n = 3). (E) CD8αα^{+}TCRγδ^{+} and CD8αα^{+}TCRαβ^{+} IELs of control, Vil-Cre IL-15cKO, and Bcl-2 Vil-Cre IL-15cKO mice were stained with annexin V and propidium iodide (PI) and analyzed by flow cytometry. (F) Percentages of annexin V^{+} PI^{-} early apoptotic cells in CD8αα^{+}TCRγδ^{+} and CD8αα^{+}TCRαβ^{+} IELs were calculated (n = 3). Student's *t*-tests for unpaired data were used to compare values between two groups. (G) Expression of Fas and (H) CD122 on CD8αα^{+}TCRαβ^{+} and CD8αα^{+}TCRγδ^{+} IELs cells of Vil-Cre IL-15cKO mice or Bcl-2 Vil-Cre IL-15cKO mice. Data are representative of two independent experiments. Student's *t*-tests for unpaired data were used to compare values between two groups. *, $p < 0.05$; n.s., not significant.

Figure 6. IEC-derived IL-15 is required for functional maturation of CD8αα IELs.

(A) Freshly isolated IELs from control or Vil-Cre IL-15cKO mice were surface stained with anti-TCRγδ, anti-TCRαβ, anti-CD4, anti-CD8α, anti-CD8β Abs and then subjected to intracellular staining for granzyme B. Representative FACS plot of granzyme B expression in CD8αα^{+}TCRαβ^{+} and CD8αα^{+}TCRγδ^{+} IELs are shown. (B) Percentages of granzyme B producing cells of CD8αα^{+}TCRαβ^{+} and CD8αα^{+}TCRγδ^{+} IELs of control or Vil-Cre IL-15cKO mice are shown (n = 3). (C) RT-qPCR analysis of granzyme B transcripts in sorted

IEL subsets. Transcript levels were normalized to HPRT (n = 3). (D) Flow cytometry analysis and (E) mean fluorescence intensity (MFI) of PD-1 expression on CD8αα IELs of control and Vil-Cre IL-15cKO mice (n = 3). (F) Flow cytometry profiles for granzyme B and PD-1 expression on $CD8\alpha\alpha^{+}TCR\gamma\delta^{+}$ and $CD8\alpha\alpha^{+}TCR\alpha\beta^{+}$ IELs of control and Vil-Cre IL-15cKO mice were shown. (G) Absolute numbers of the indicated CD8αα IEL subsets were calculated (n = 3). Student's *t*-tests for unpaired data were used to compare values between two groups. *, $p < 0.05$; n.s., not significant.

Figure 1

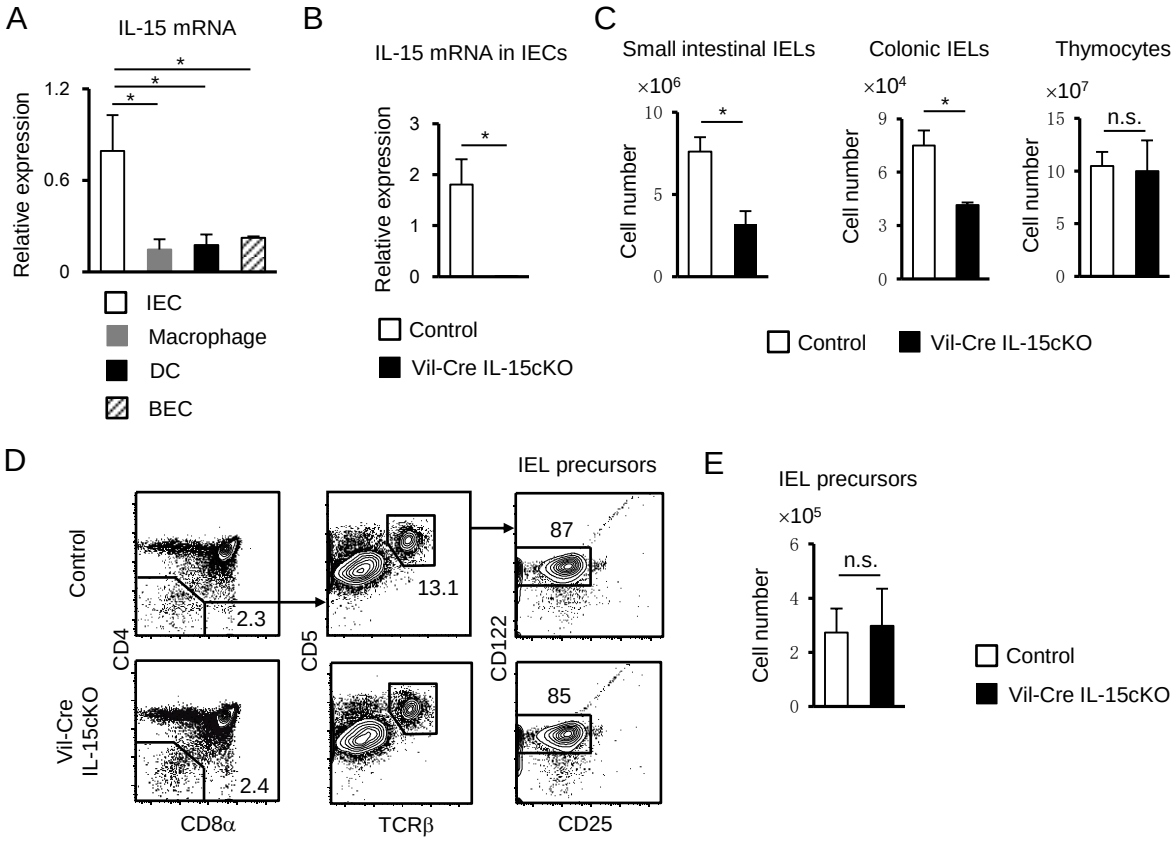

Figure 2

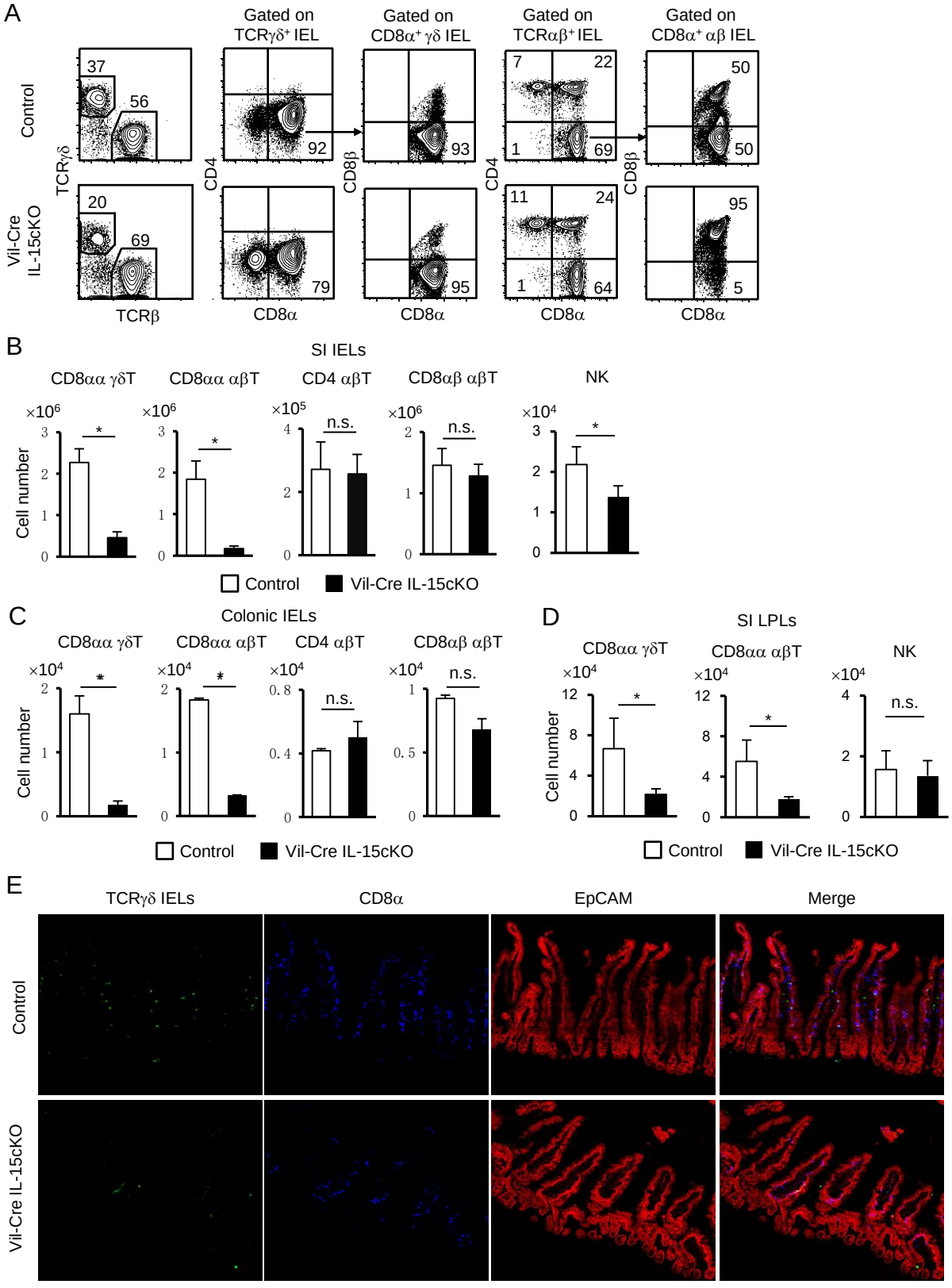

Figure 3

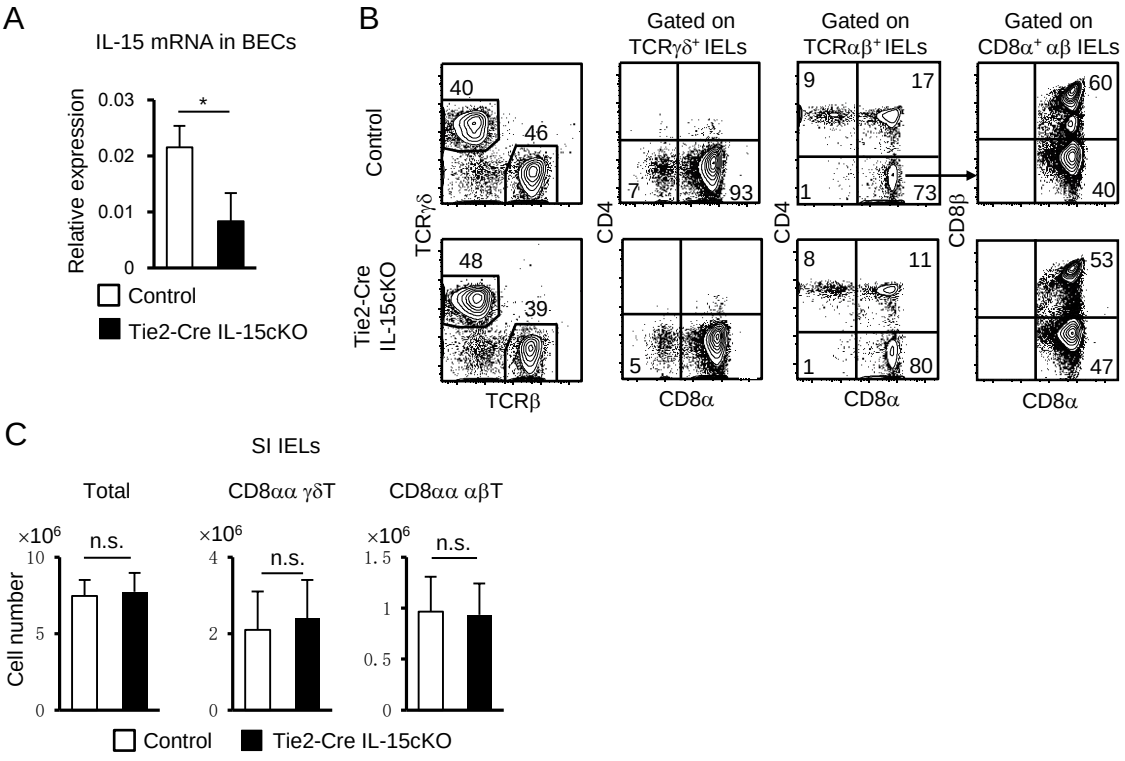

Figure 4

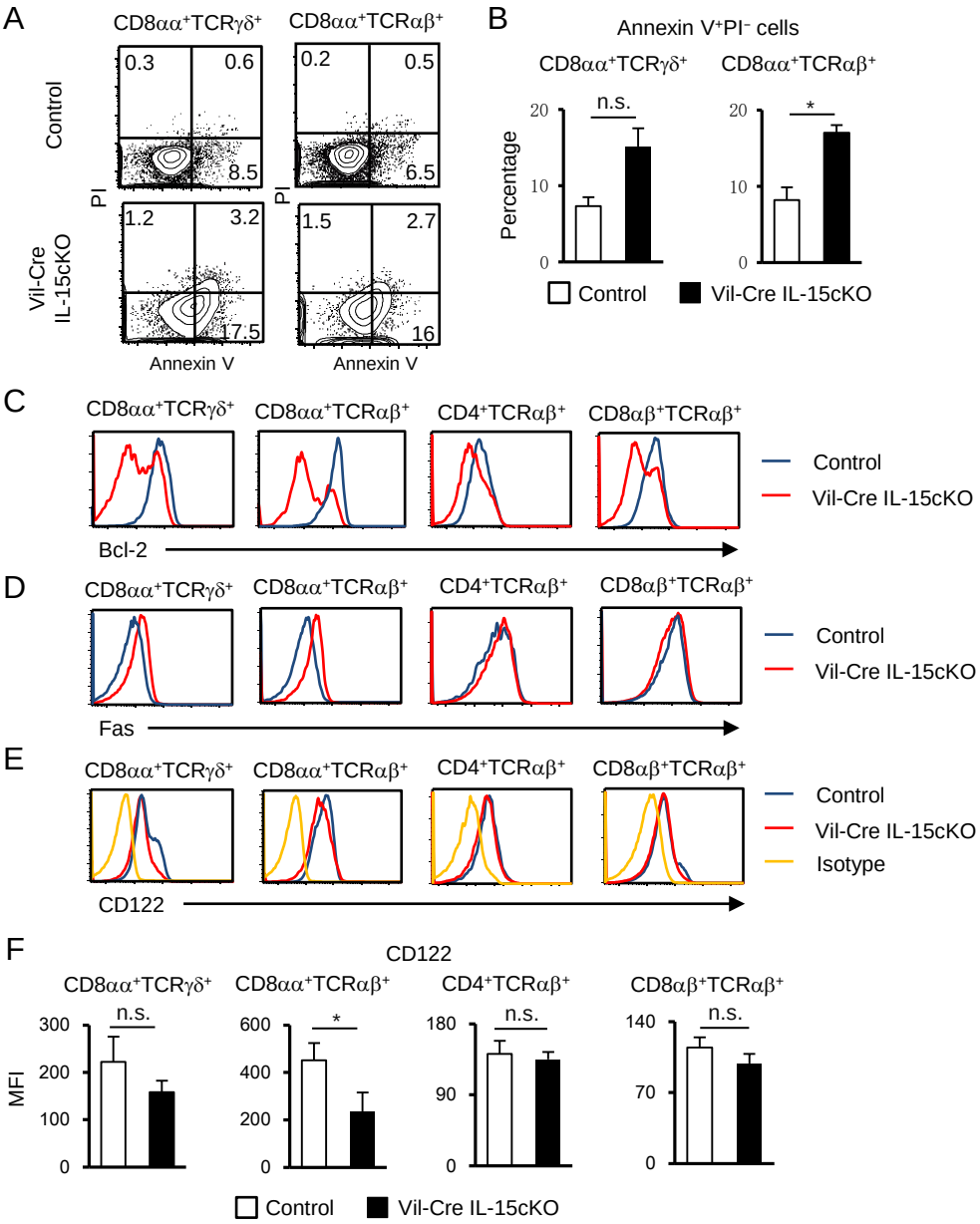

Figure 5

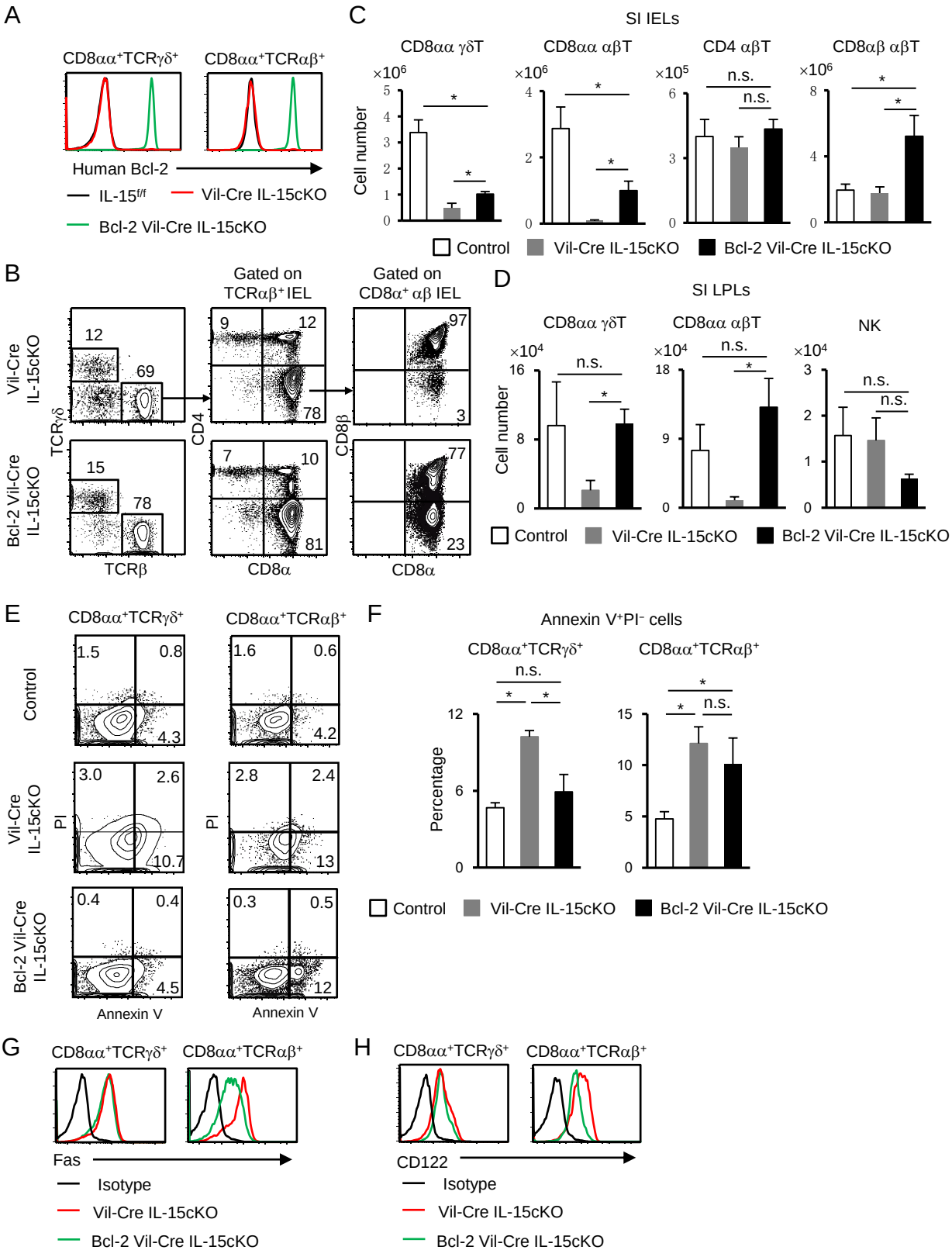

Figure 6

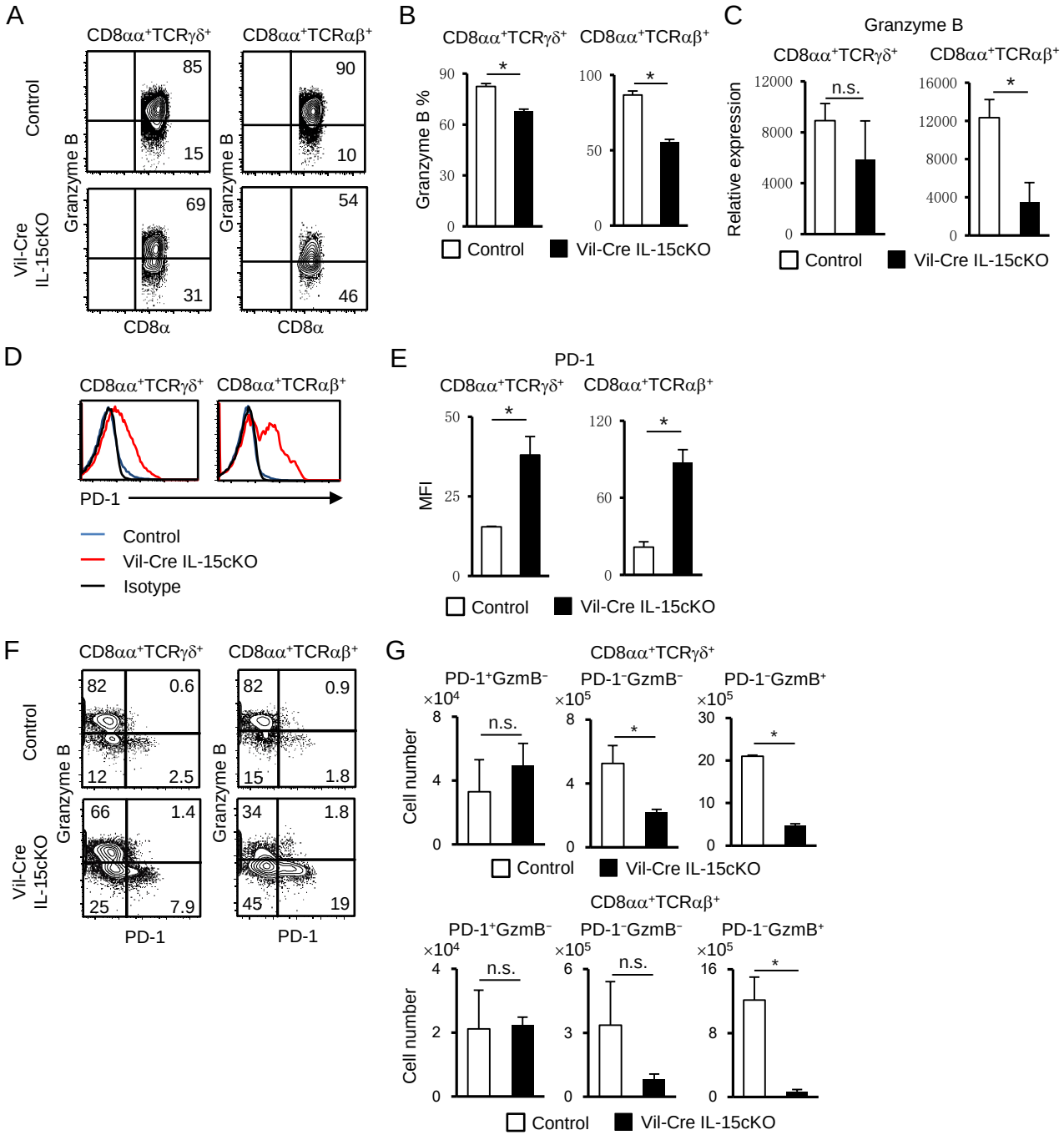

Supplementary Figure Legends

Figure S1. NK cells in lamina propria are independent on IEC-derived IL-15, but dependent on APC- or BEC-derived IL-15.

NK cells in LPLs were analyzed as $CD3^{-}NK1.1^{+}CD27^{+}CD127^{-}$ by flow cytometry. Percentages and absolute numbers of lamina propria NK cells in (A) Vil-Cre IL-15cKO (n = 3), (B) LysM-Cre IL-15cKO (n = 4), (C) CD11c-Cre IL-15cKO (n = 3) and (D) Tie2-Cre IL-15cKO (n = 2) mice were shown. Student's *t*-tests for unpaired data were used to compare values between two groups. *, $p < 0.05$; n.s., not significant.

Figure S2. Gut microbiota is not altered in Vil-Cre IL-15cKO mice.

Gut microbiota was analyzed in feces samples of control and Vil-Cre IL-15cKO mice. Relative bacterial abundance (A) was classified at the family level. Comparison of alpha diversity (B) indexes between control and Vil-Cre IL-15cKO mice were shown. Chao1 and Shannon indices were used to determine the richness and diversity of the bacterial community, respectively. Beta diversity (C) in groups categorized by control and Vil-Cre IL-15cKO mice was assessed by weighted and unweighted principal coordinate analysis (PCoA).

Figure S3. DSS-induced colitis is unchanged in Vil-Cre IL-15cKO mice.

Control and Vil-Cre IL-15cKO mice were administered with 2.5% DSS in drinking water. Body weight (A) and feces score (B) were monitored every day. The values for

body weight are expressed as percentage of the body weight on day 0 (n = 8). (C) The caecum and colon were obtained from DSS-treated control and Vil-Cre IL-15cKO mice, and colon lengths were measured (n = 6). (D) Histological sores of the colon in DSS-treated mice are shown (n = 5). Every sample is evaluated by two independent evaluators, and the results are shown as average of their scores. Student's *t*-tests for unpaired data were used to compare values between two groups. (E) Colon samples from control or Vil-Cre IL-15cKO mice after DSS treatment were stained with DAPI (blue) and anti-EpCAM (red) antibody. White arrows indicate ulcer lesions. (F) Hematoxylin and eosin staining of colon sections from control and Vil-Cre IL-15cKO mice. (G) IL-15 mRNA expression was detected in colonic IECs of DSS-untreated control or DSS-treated control and Vil-Cre IL-15cKO mice by qRT-PCR and normalized to those of HPRT (n = 3). Percentage of IFN-γ^+ CD4 T cells (H) and cell number of NK cells (I) in colonic lamina propria of control and Vil-Cre IL-15cKO mice after DSS treatment were shown (n = 3). Student's *t*-tests for unpaired data were used to compare values between two groups. *, $p < 0.05$; n.s., not significant.

Figure S4. CD122^{hi} and CD122^{lo} subsets of CD8αα$^+$TCRαβ$^+$ IELs show different proliferation abilities.

(A) Ki67 expression on CD8αα$^+$TCRαβ$^+$ IELs of control or Vil-Cre IL-15cKO mice. Proliferation of lymphocytes was represented with ratio of Ki67$^+$ cells. (B)

CD8αα^{+}TCRαβ^{+} IELs were divided into CD122^{lo} and CD122^{hi} subsets. Proliferation of each subset is shown. Data are representative of two independent experiments.

Figure S1

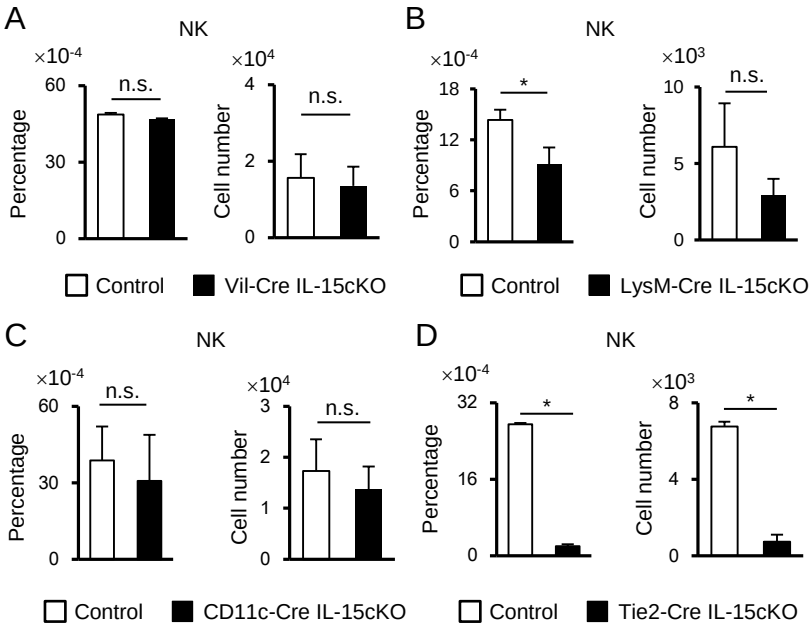

Figure S2

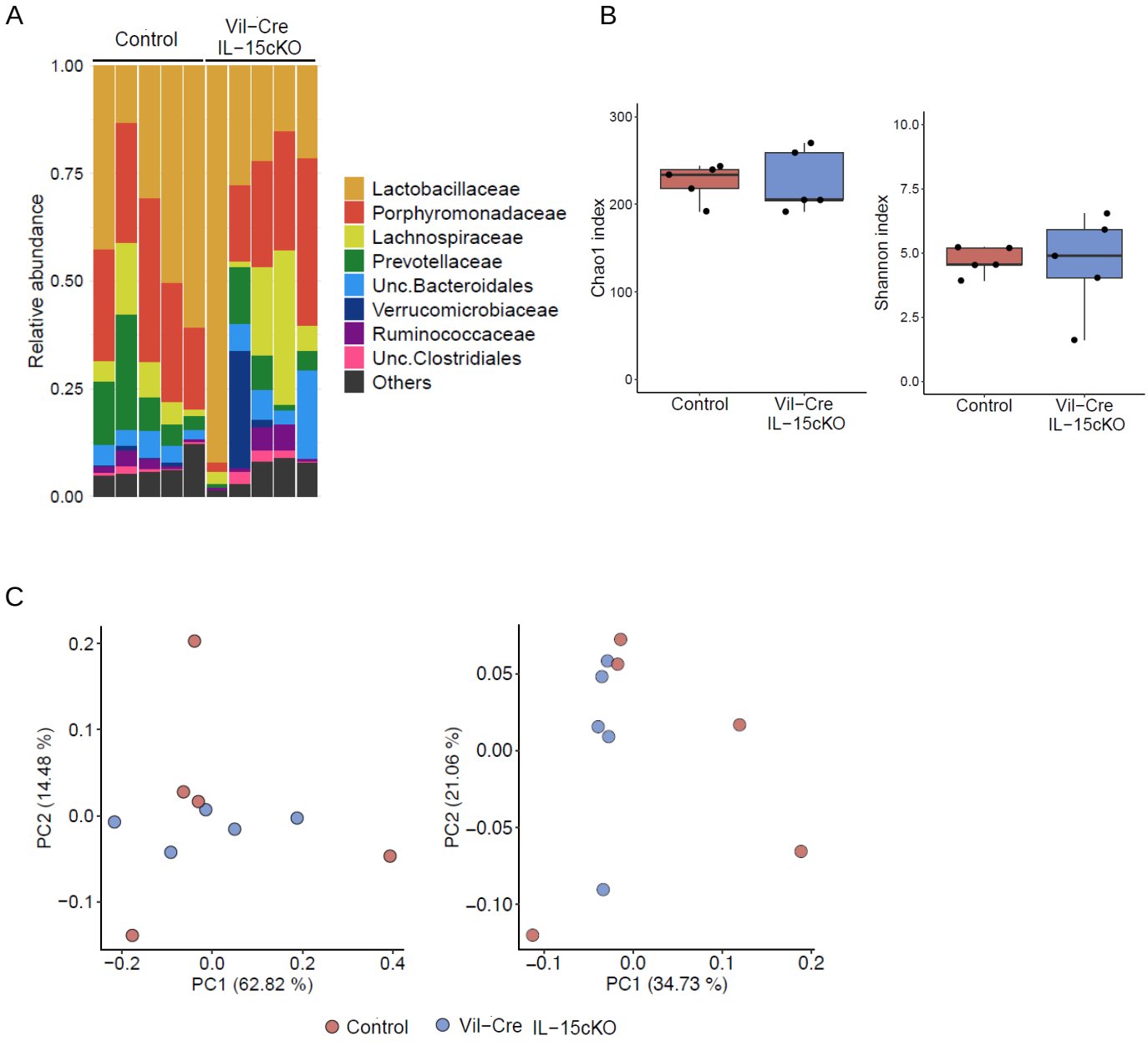

Figure S3

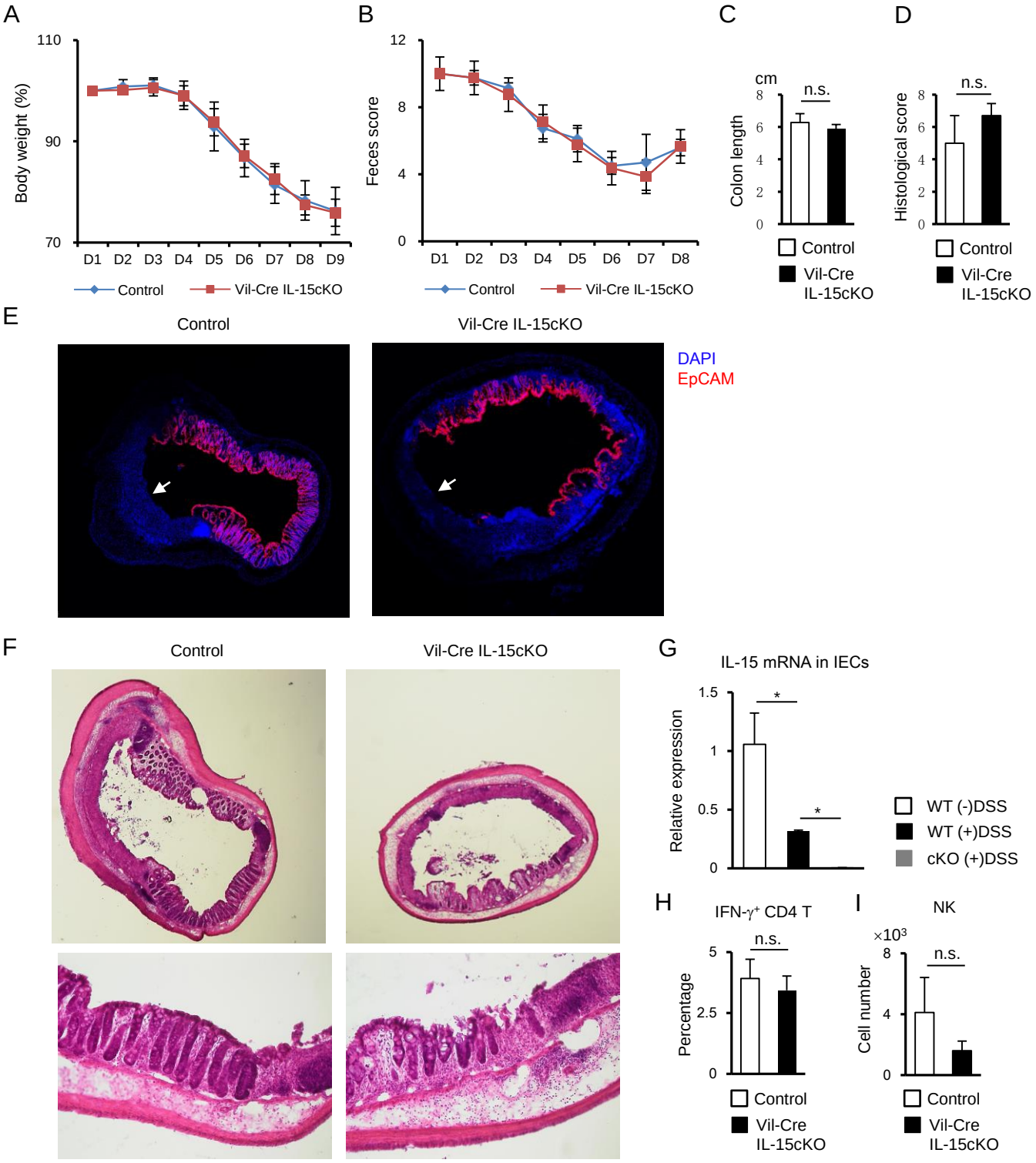

Figure S4